Supporting Information

Self-sorting of crown ether/secondary ammonium ion hetero-[*c*2]daisy chain pseudorotaxanes

Bo Zheng,[a] Fabian Klautzsch,[b] Min Xue,[a] Feihe Huang,[a]
Christoph A. Schalley*[b],

[a] *State Key Laboratory of Chemical Engineering, Department of Chemistry, Zhejiang University, Hangzhou 310027, P. R. China, fhuang@zju.edu.cn*

[b] *Institut für Chemie und Biochemie, Freie Universität Berlin, Takustr. 3, 14195 Berlin, Germany, c.schalley@fu-berlin.de*

Table of Contents

1. NMR Spectra of $2{\cdot}PF_6$, $3{\cdot}PF_6$ and $4{\cdot}PF_6$

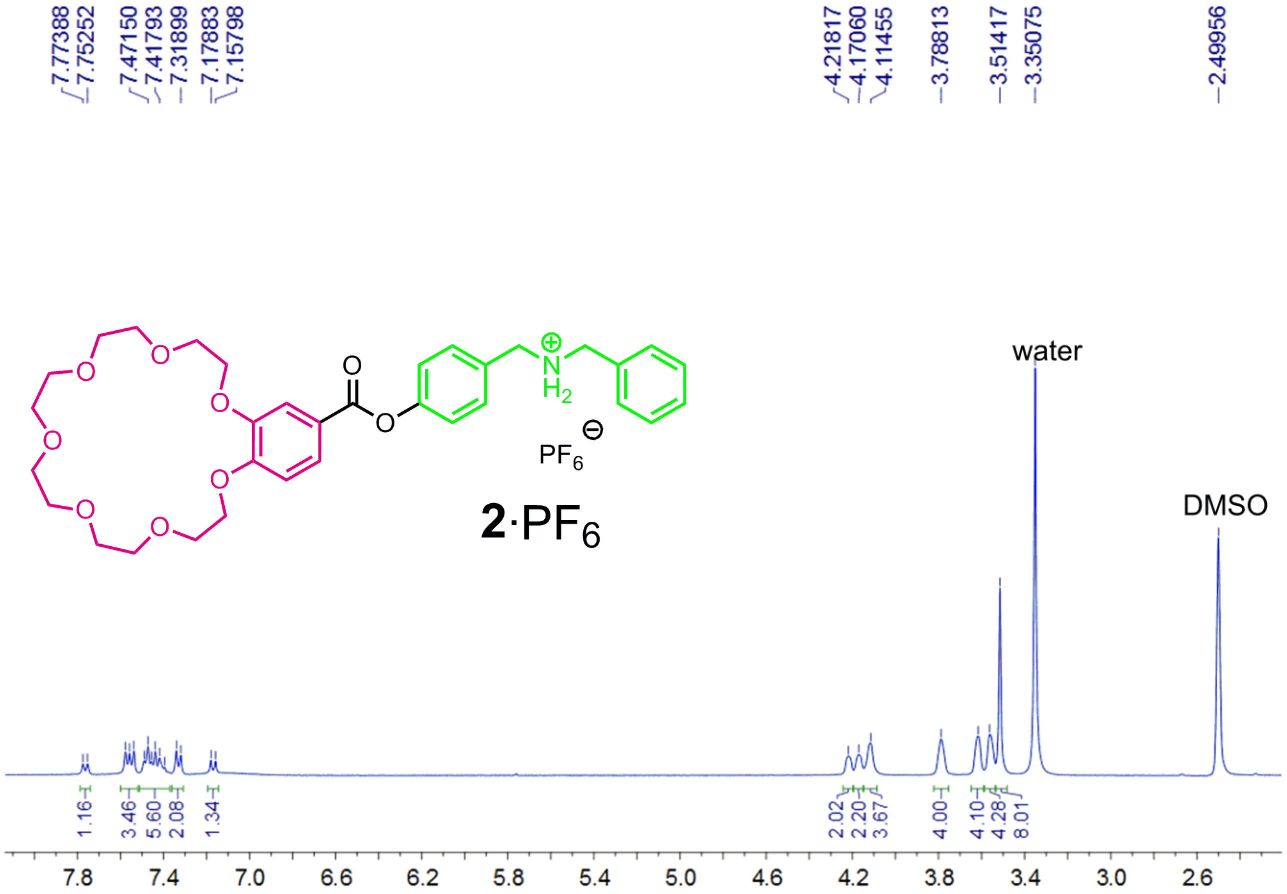

Figure S1. ^{1}H NMR spectrum (500 MHz, DMSO-d_6, 295K) of **2**$\cdot PF_6$.

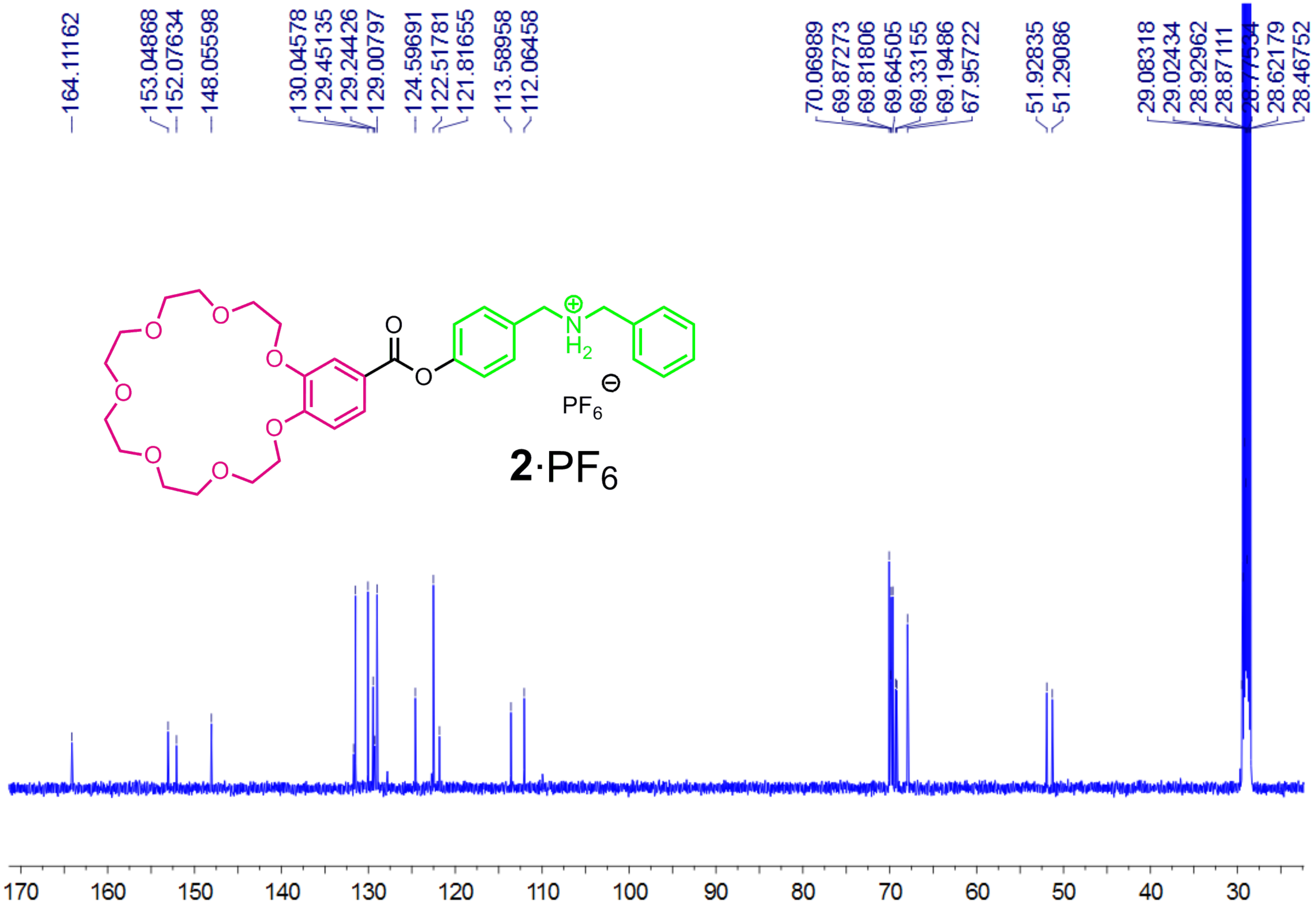

Figure S2. ^{13}C NMR spectrum (125 MHz, acetone-d_6, 295K) of **2**·PF_6.

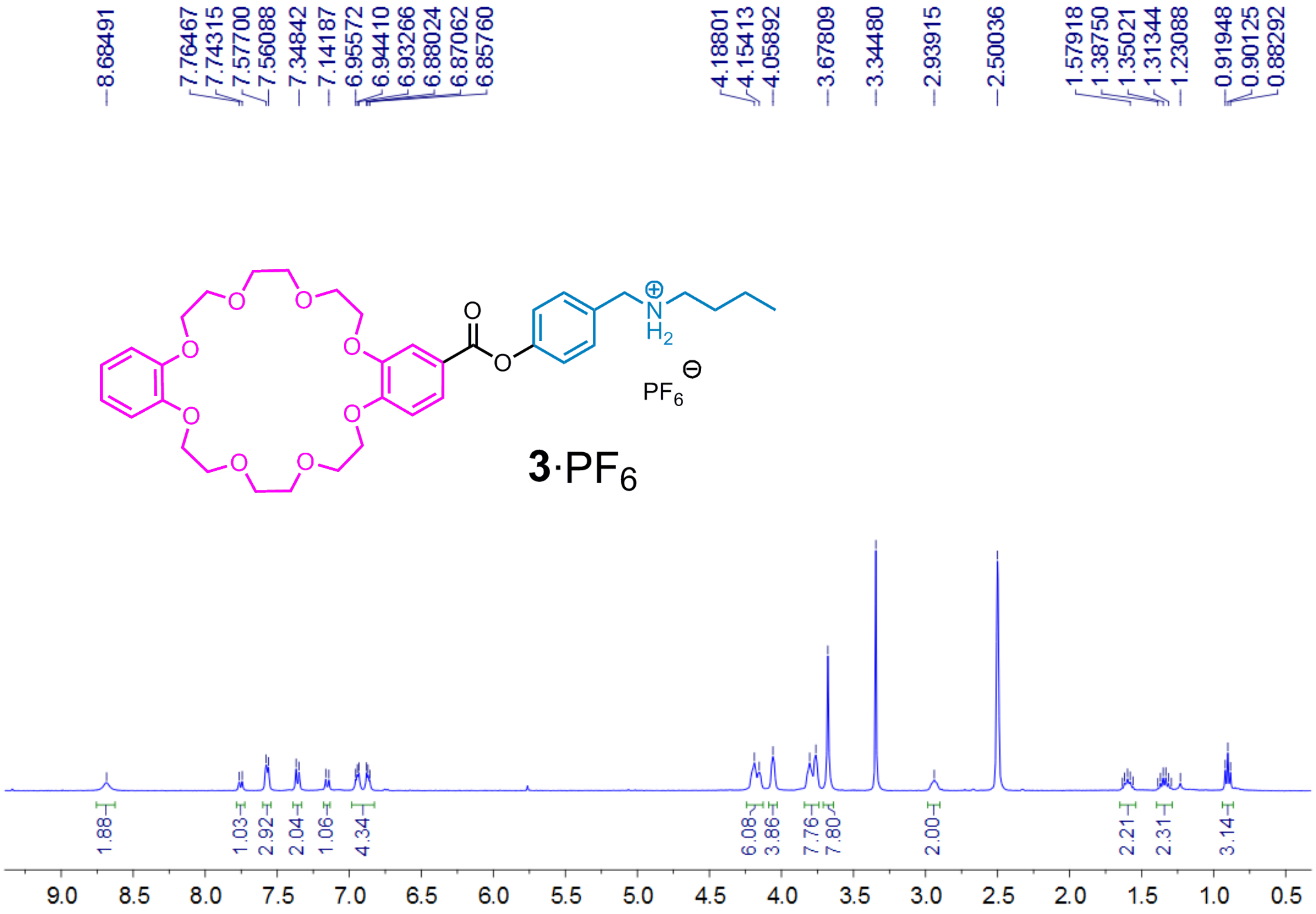

Figure S3. ^{1}H NMR spectrum (500 MHz, DMSO-d_6, 295K) of **3**·PF_6.

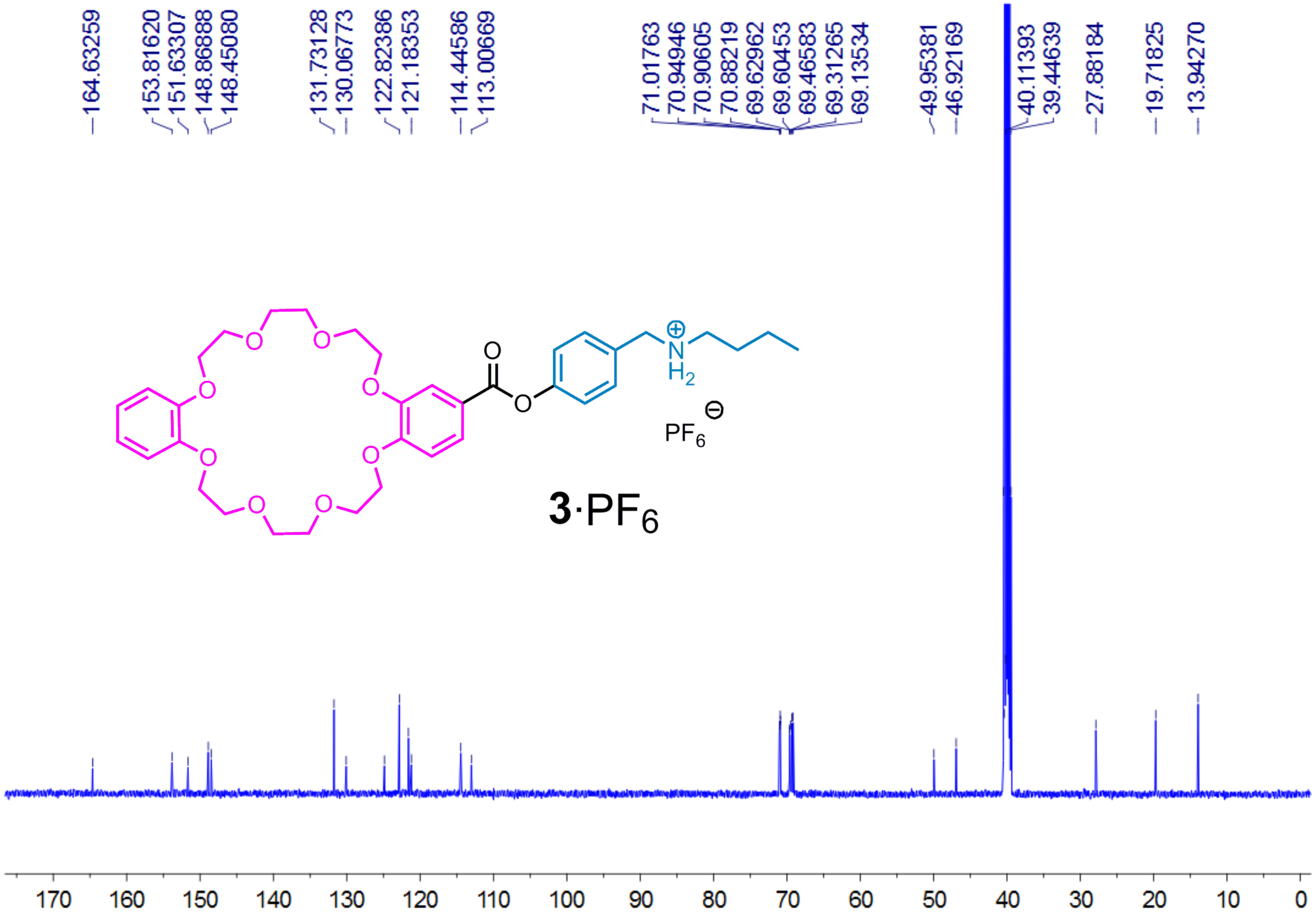

Figure S4. ^{13}C NMR spectrum (125 MHz, DMSO-d_6, 295K) of **3**·PF_6.

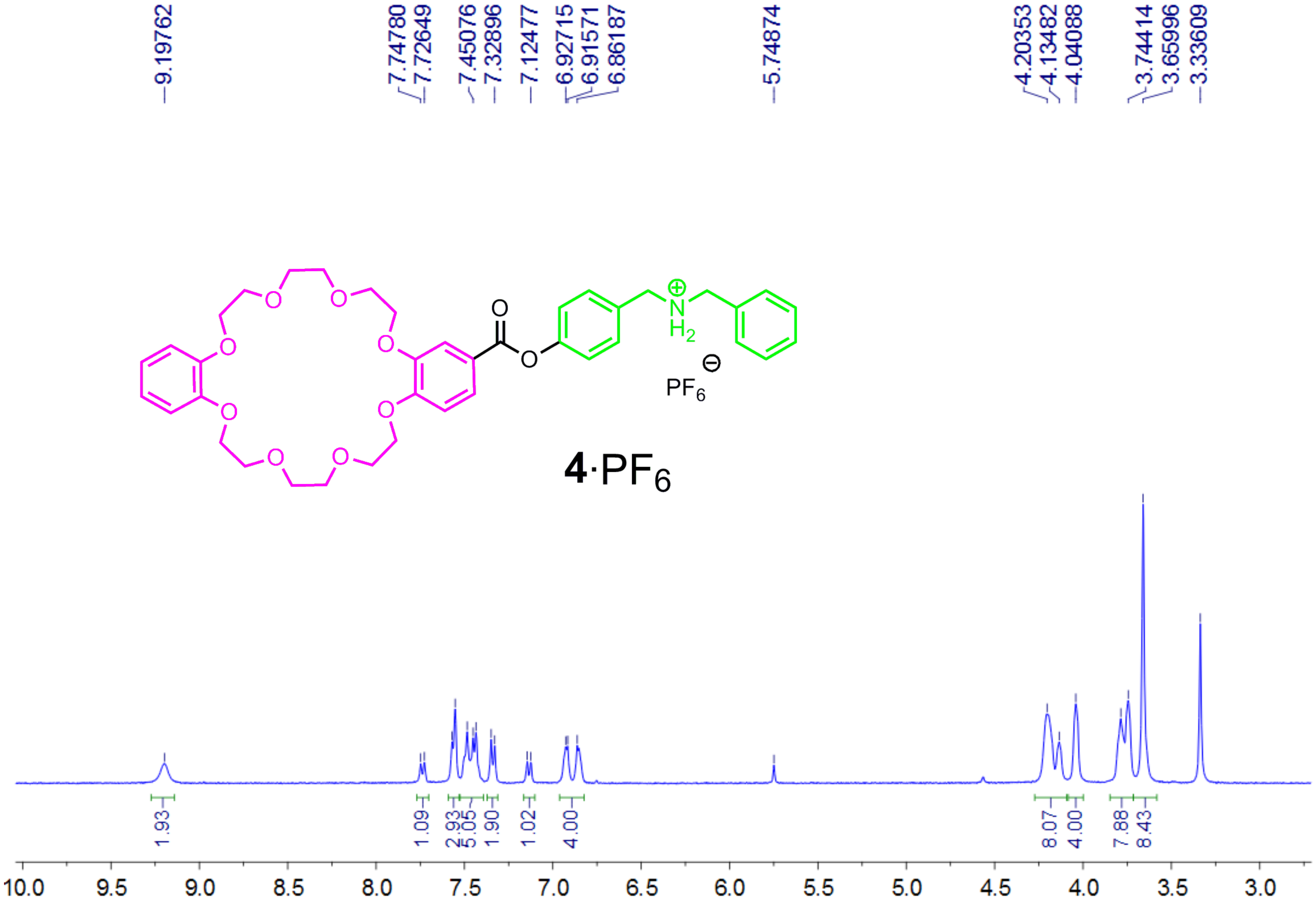

Figure S5. ^{1}H NMR spectrum (500 MHz, DMSO-d_6, 295K) of **4**·PF_6.

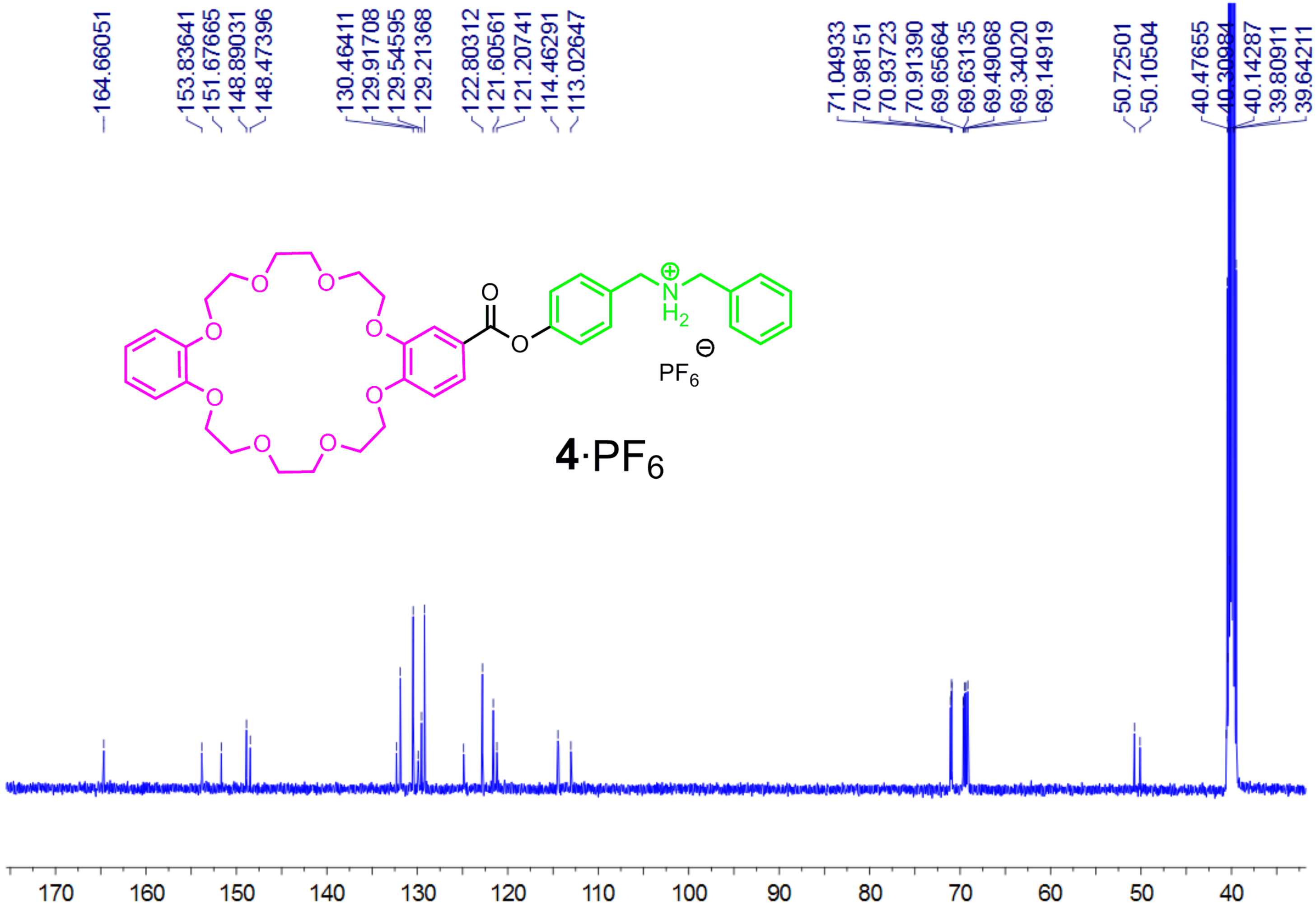

Figure S6. ^{13}C NMR spectrum (125 MHz, DMSO-d_6, 295K) of **4**·PF_6.

2. Comparison of the ^{1}H NMR Spectra of 1·PF_6, 2·PF_6, 3·PF_6 and 4·PF_6

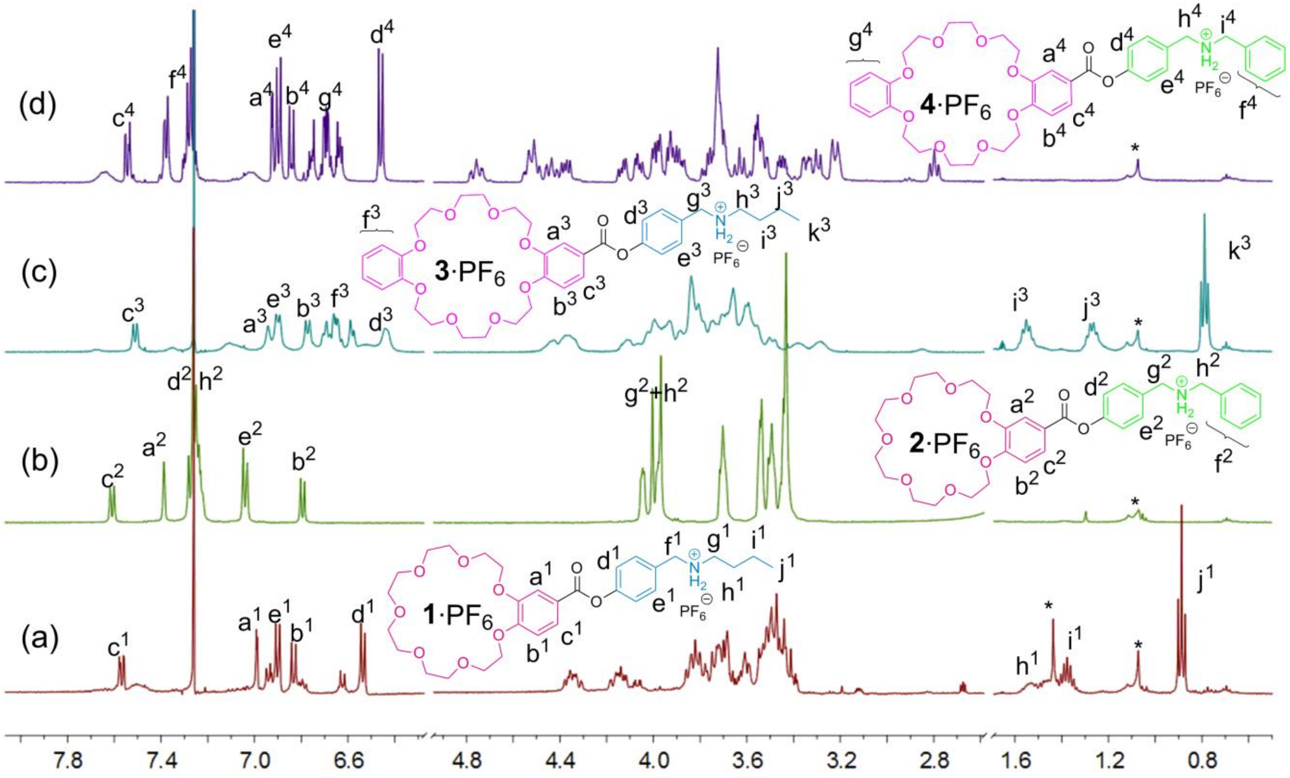

Figure S7. ^{1}H NMR spectra (500 MHz, $CDCl_3$: CD_3CN = 2:1, 10.0 mM, 298K) of (a) **1**·PF_6, (b) **2**·PF_6, (c) **3**·PF_6 and (d) **4**·PF_6. Asterisks indicate solvent impurities.

The ^{1}H NMR spectra of **1**·PF_6, **3**·PF_6 and **4**·PF_6 are much more complicated as compared to that of **2**·PF_6. In particular, most of the CH_2 groups appear with two sets of signals indicating the presence of diastereotopic protons, although the monomers are achiral. This is only consistent with the formation of complexes, the simplest of which is the daisy chain dimer. Instead, **2**·PF_6 cannot form a dimer structure due to the size misfit of the larger benzylic stopper group and the smaller crown ether. Only one set of signals is thus observed. These results provide evidence for homodimeric daisy chain formation from monomers, **1**·PF_6, **3**·PF_6 and **4**·PF_6 in $CDCl_3$/CD_3CN (2:1) solution.

3. ^{1}H NMR Spectra of 1·PF$_6$ and 1·PF$_6$/KPF$_6$, and ^{1}H-^{1}H COSY NMR Spectrum of 1·PF$_6$

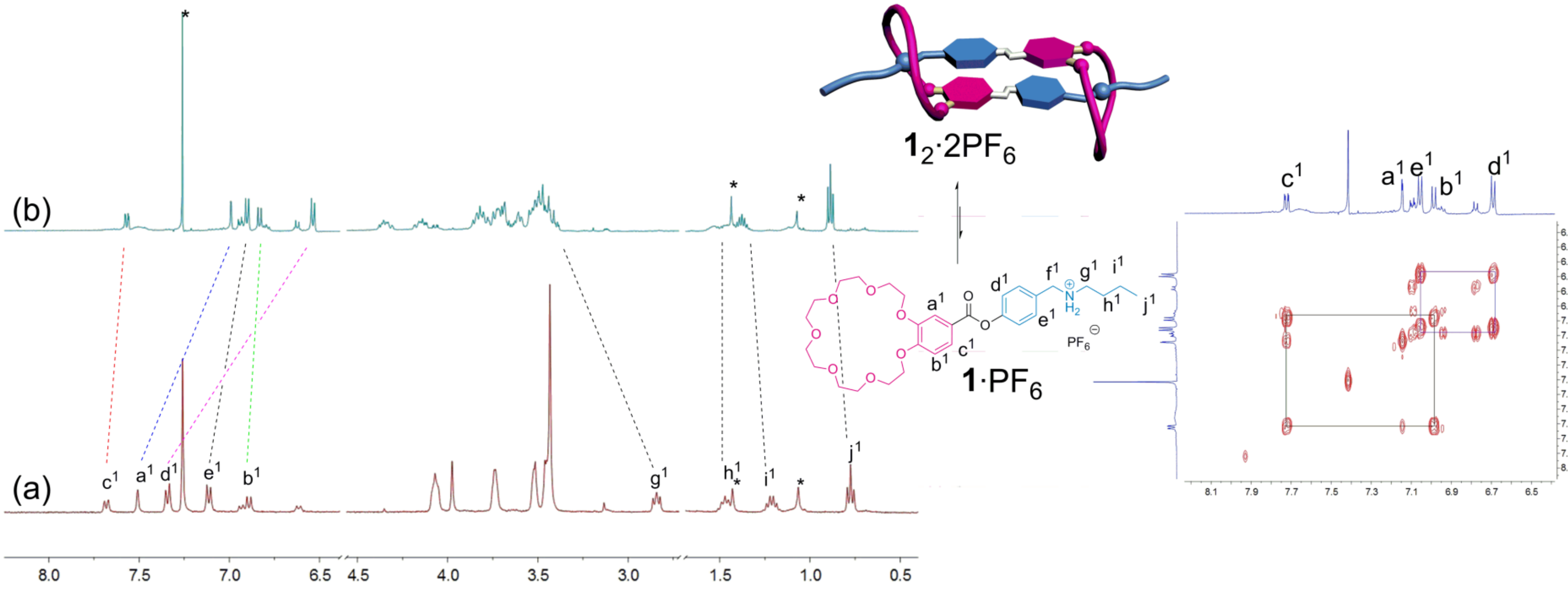

Figure S8. ^{1}H NMR spectra (500 MHz, $CDCl_3$:CD_3CN = 2:1, 10.0 mM, 298K) of (a) **1**·PF$_6$ with excess KPF$_6$ and (b) **1**·PF$_6$. Inset: partial ^{1}H-^{1}H COSY NMR spectrum of **1**·PF$_6$ (8.1–6.5 ppm). Asterisks indicate solvent impurities. The crown ether rings are occupied by K$^+$, so that no threaded structure can form. The spectrum of the potassiated monomer therefore contains only one set of signals. Without KPF$_6$ added, the complexation-induced signal shifts are typical for threaded ammonium ions and suggest the formation of [*c*2]daisy chain complexes in agreement with the results discussed above (Figure S7).

4. ^{1}H NMR Spectra of 2·PF_6 and 2·PF_6/KPF_6

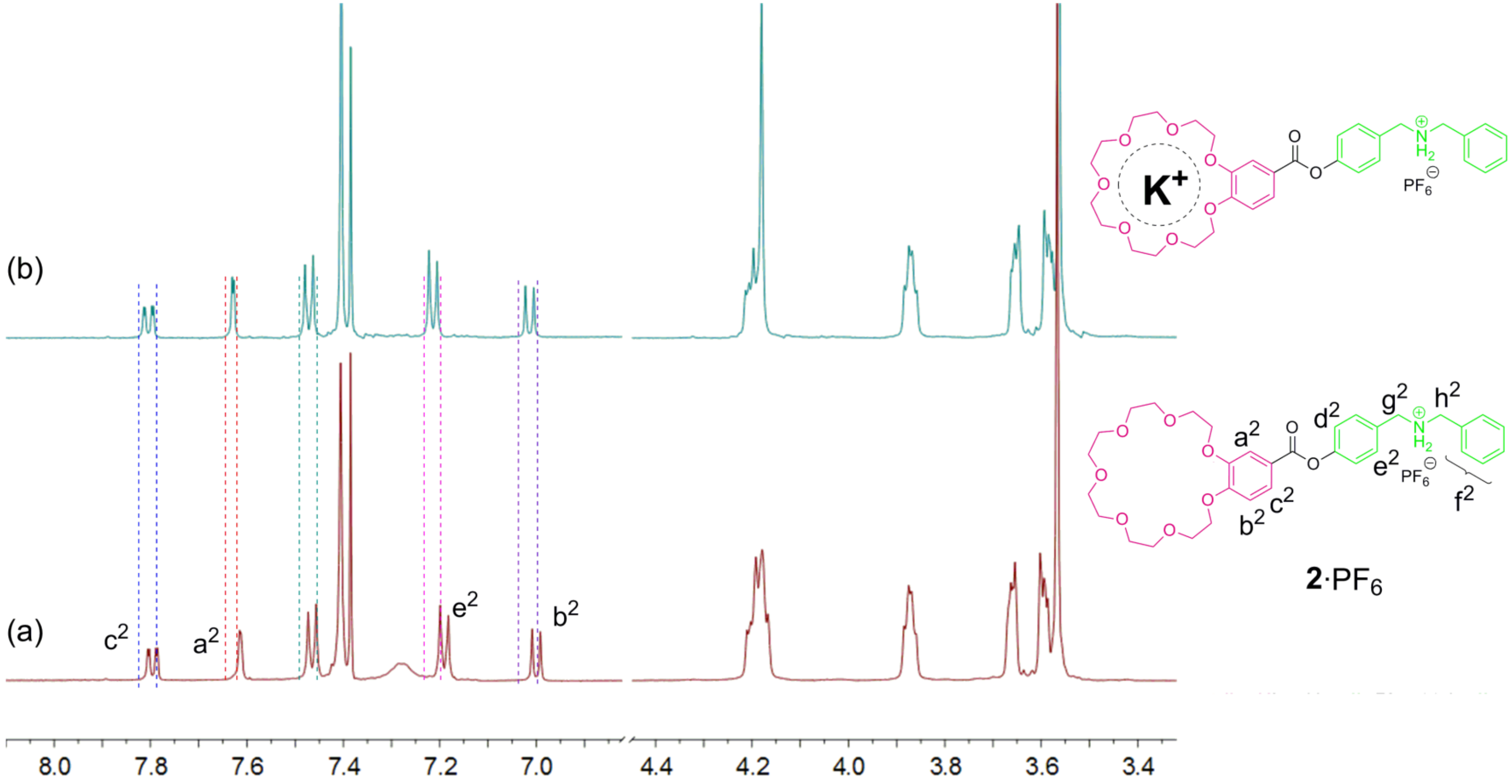

Figure S9. ^{1}H NMR spectra (500 MHz, $CDCl_3$:CD_3CN = 2:1, 10.0 mM, 298K) of (a) **2**·PF_6 and (b) **2**·PF_6 with excess KPF_6.

5. ^{1}H NMR Spectra of 3·PF$_6$ and 3·PF$_6$/KPF$_6$, and ^{1}H-^{1}H COSY NMR Spectrum of 3·PF$_6$

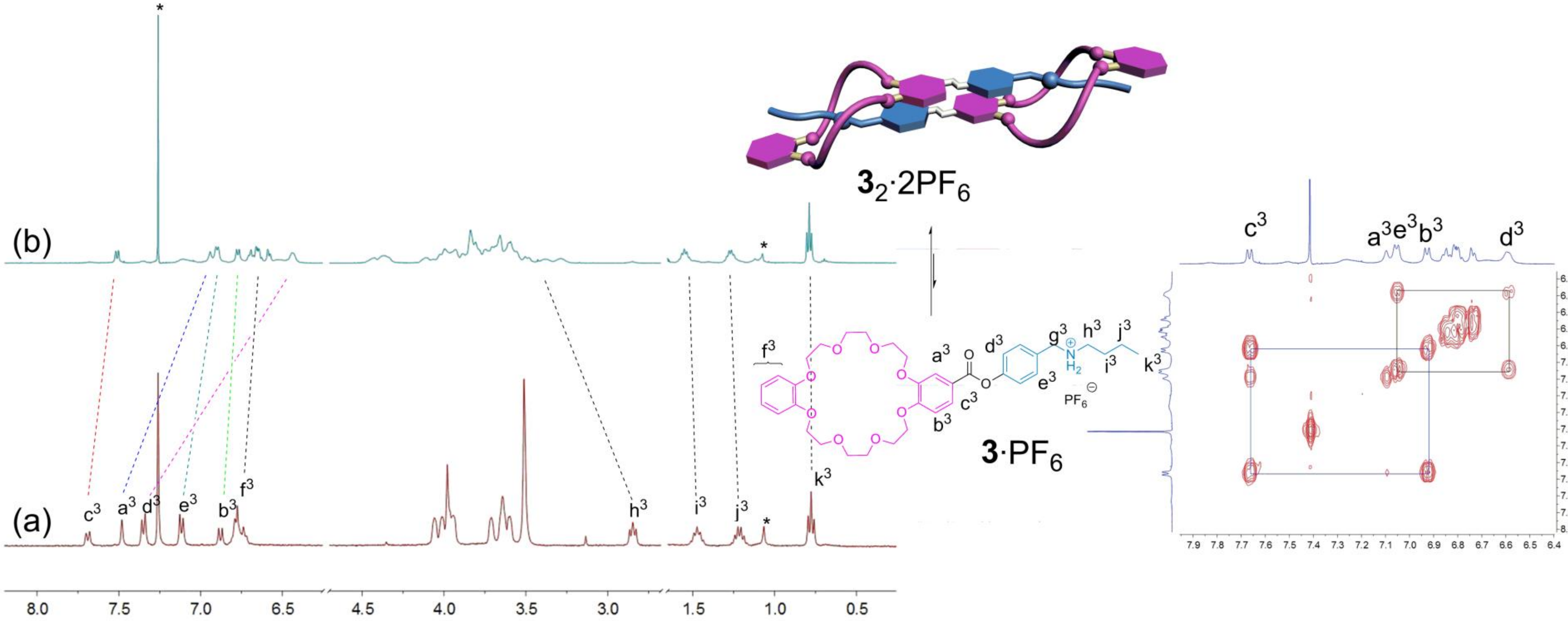

Figure S10. ^{1}H NMR spectra (500 MHz, $CDCl_3$:CD_3CN = 2:1, 10.0 mM, 298K) of (a) **3**·PF$_6$ with excess KPF$_6$ and (b) **3**·PF$_6$. Inset: partial ^{1}H-^{1}H COSY NMR spectrum of **3**·PF$_6$ (7.9–6.4 ppm). Asterisks indicate solvent impurities. The behavior is analogous to that of **1**·PF$_6$ so that daisy chain formation is again supported for the potassium free sample as discussed above (Figures S7 and S8).

6. ^{1}H NMR Spectra of 4·PF$_6$ and 4·PF$_6$/KPF$_6$, and ^{1}H-^{1}H COSY NMR Spectrum of 4·PF$_6$

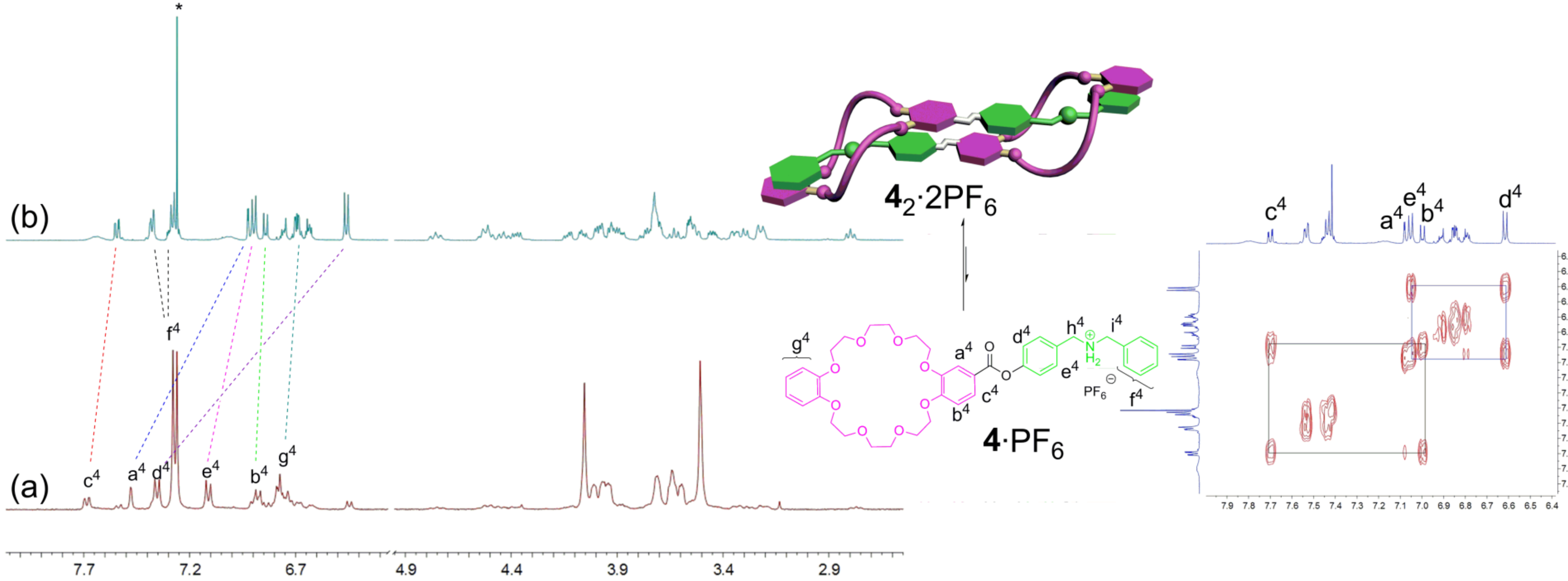

Figure S11. ^{1}H NMR spectra (500 MHz, CDCl$_3$:CD$_3$CN = 2:1, 10.0 mM, 298K) of (a) **4**·PF$_6$ with excess KPF$_6$ and (b) **4**·PF$_6$. Inset: partial ^{1}H–^{1}H COSY NMR spectrum of **4**·PF$_6$ (7.9–6.4 ppm). The behavior is analogous to those of **1**·PF$_6$ and **3**·PF$_6$ so that daisy chain formation is again supported for the potassium free sample as discussed above (Figures S7, S9 and S10).

7. ESI Mass Spectra of a Mixture of $1_2{\cdot}2PF_6$ and $4_2{\cdot}2PF_6$

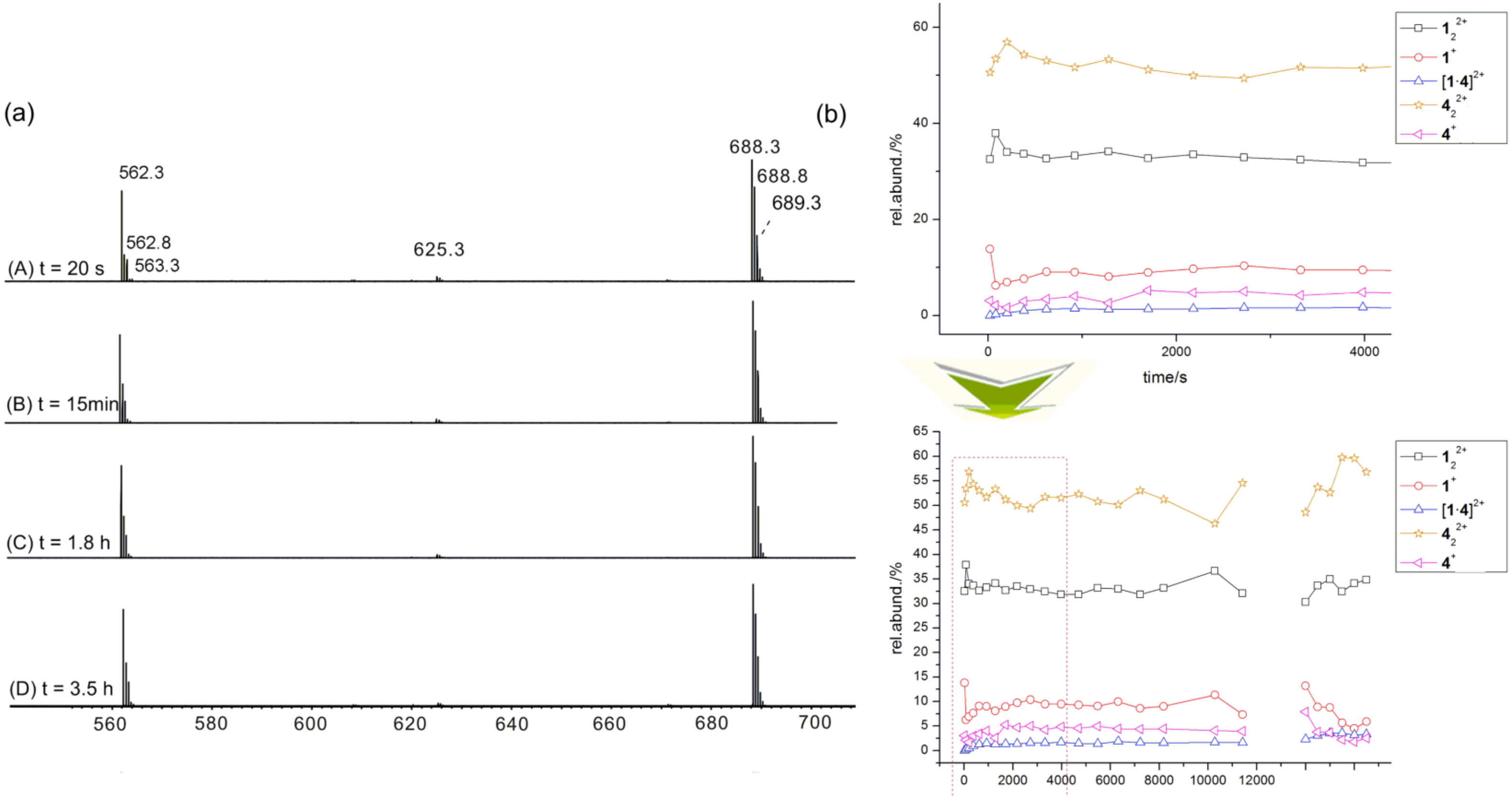

Figure S12. a) Mass spectra and b) time-plot of complex formation in a mixture of $\mathbf{1_2}{\cdot}2PF_6$ and $\mathbf{4_2}{\cdot}2PF_6$. Even at longer reaction intervals, no heterodimeric daisy chain forms.

8. ^{1}H NMR Spectra of a Mixture of $\mathbf{1}_2\cdot 2PF_6$ and $\mathbf{4}_2\cdot 2PF_6$

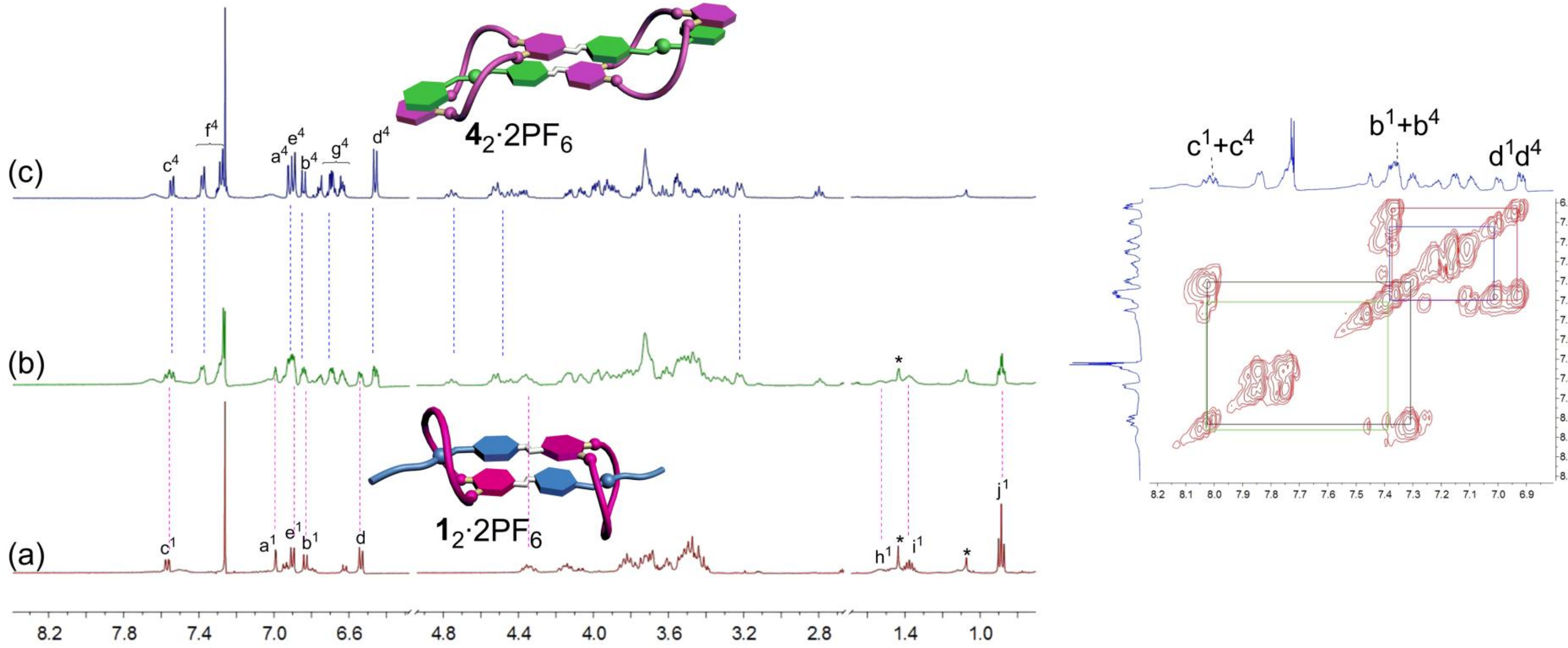

Figure S13. ^{1}H NMR spectra (500 MHz, $CDCl_3$:CD_3CN = 2:1, 10.0 mM, 298K) of (a) $\mathbf{1}\cdot PF_6$, (b) equimolar mixture of $\mathbf{1}_2\cdot 2PF_6$ and $\mathbf{4}_2\cdot 2PF_6$ and (c) $\mathbf{4}_2\cdot 2PF_6$. Inset: partial ^{1}H-^{1}H COSY NMR spectrum of the mixture (8.2–6.9 ppm). Asterisks indicate solvent impurities. Due to the similarity of the homo- and heterodimer binding motifs and spectral complexity, it is not straightforward to determine exact amounts of homo- and heterodimers present in the mixture. Nevertheless, the spectrum of the mixture is a superposition of the two spectra of the individual components in agreement with the absence of heterodimers.

9. ESI mass spectra of a Mixture of 2·PF_6 and 4_2·2PF_6

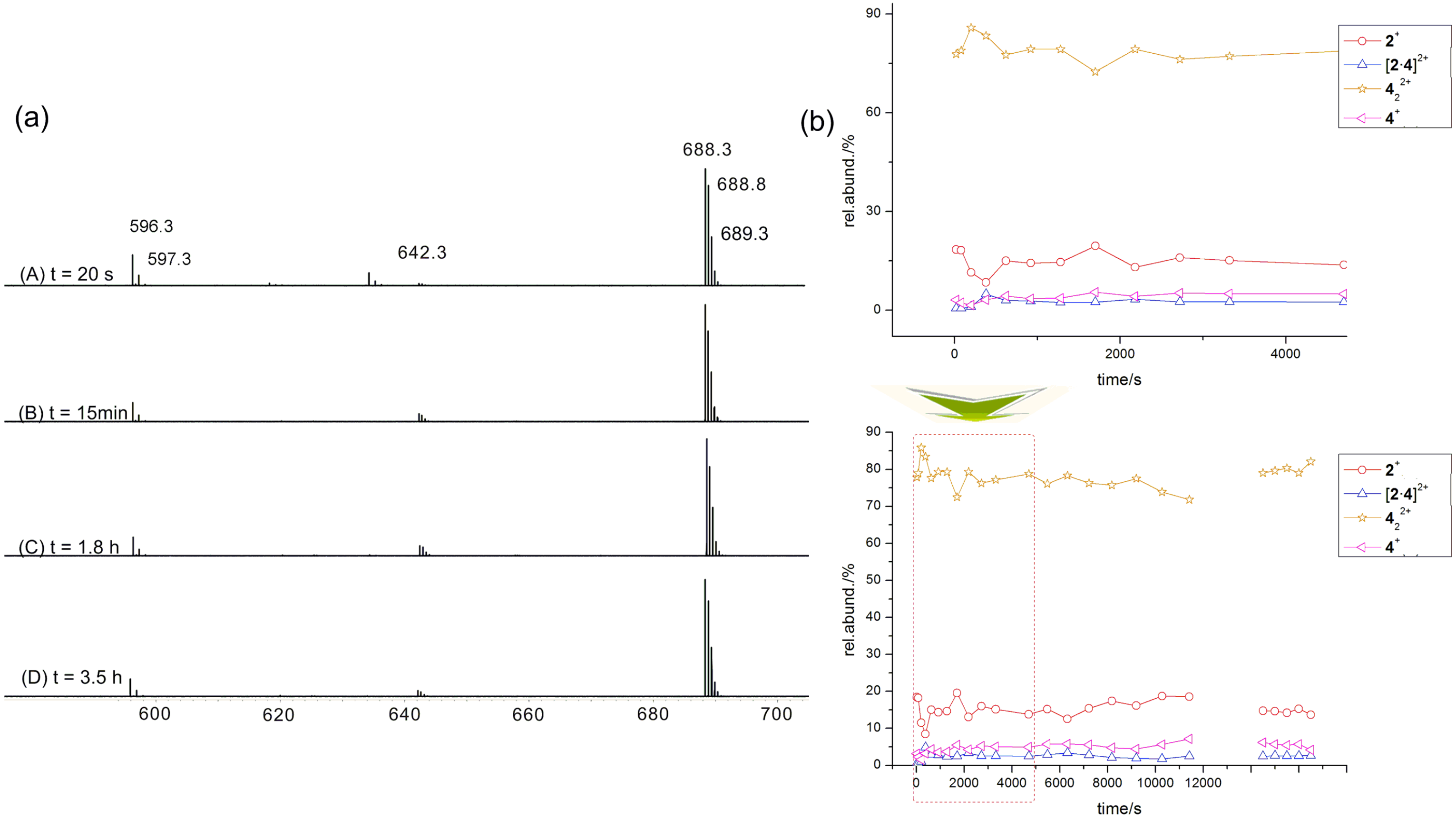

Figure S14. a) Mass spectra and b) time-plot of complex formation between **2**·PF_6 and **4_2**·PF_6. Again, no heterodimer forms even at prolonged equilibration times.

10. ^{1}H NMR Spectra of a Mixture of 2·PF$_6$ and 4$_2$·2PF$_6$

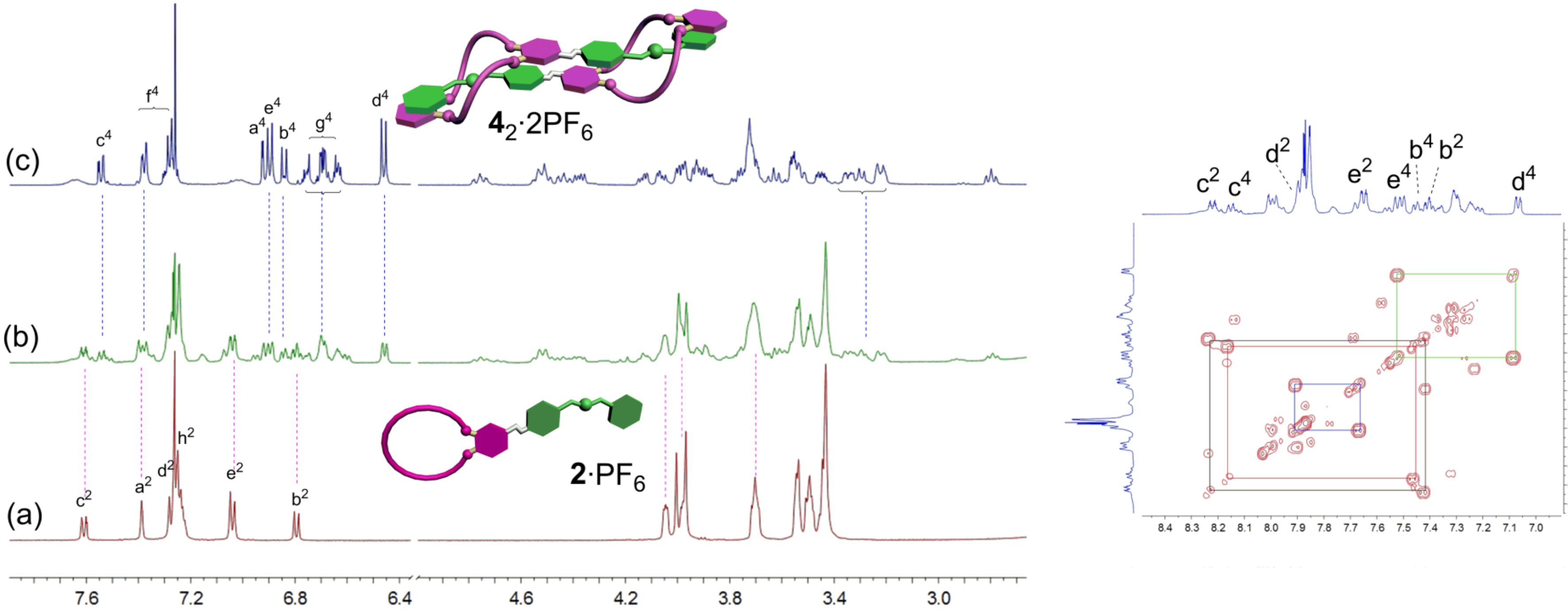

Figure S15. ^{1}H NMR spectra (500 MHz, CDCl$_3$:CD$_3$CN = 2:1, 10.0 mM, 298K) of (a) **2**·PF$_6$, (b) equimolar in monomer concentration of **2**·PF$_6$ and **4**$_2$·2PF$_6$ and (c) **4**$_2$·2PF$_6$. Inset: partial ^{1}H-^{1}H COSY NMR spectrum of the mixture (8.4–7.0 ppm)..

11. ESI mass spectra of a Mixture of $1_2{\cdot}2PF_6$ and $3_2{\cdot}2PF_6$

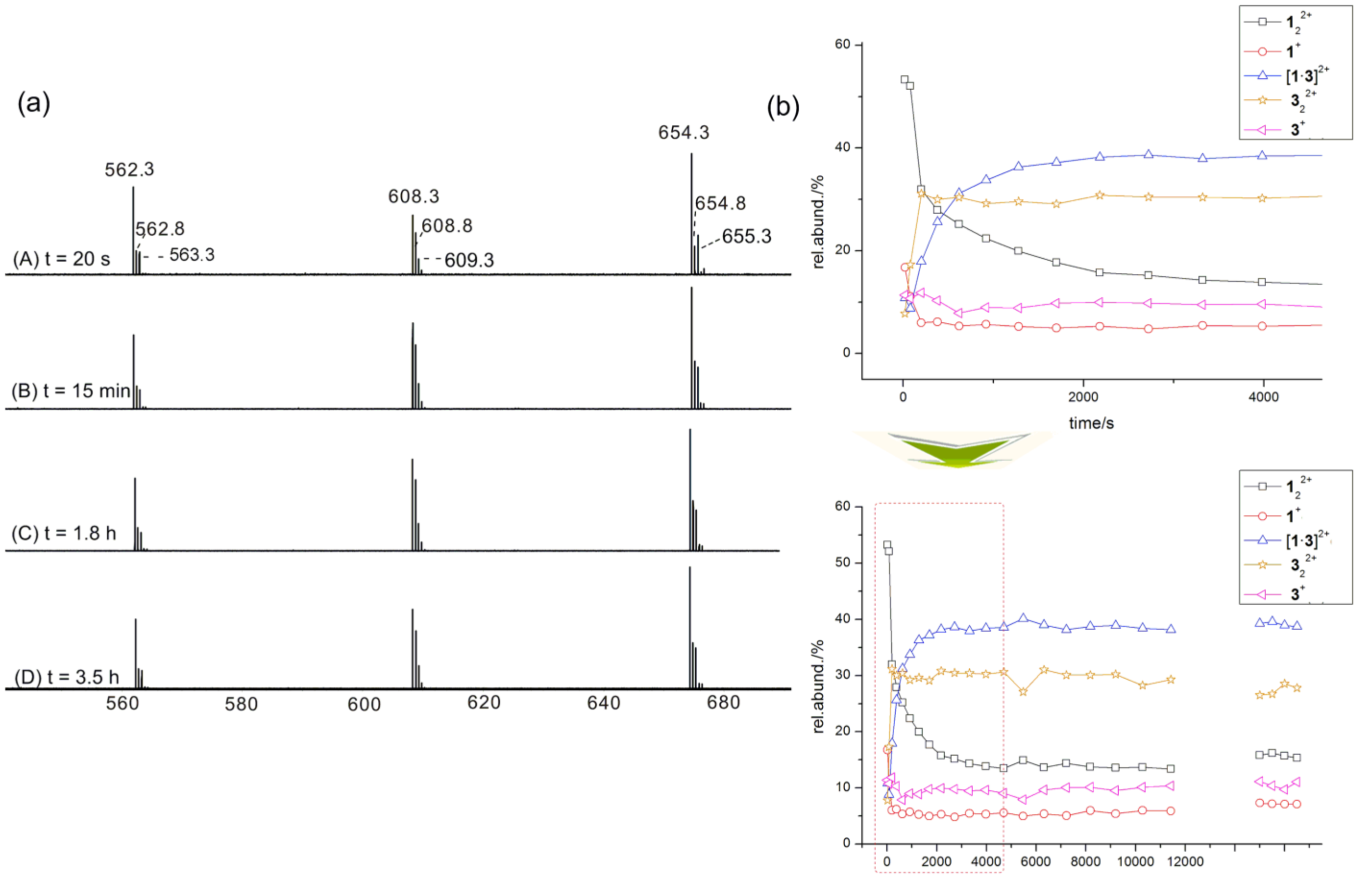

Figure S16. a) Mass spectra and b) time-plot of complex formation in the $\mathbf{1}_2{\cdot}PF_6$ and $\mathbf{3}_2{\cdot}PF_6$ mixture. As anticipated, the homodimer dications are superimposed by signals of monomers $\mathbf{1}^+$ and $\mathbf{3}^+$. The intensity ratio of the three dimeric dications is about 3:8:6 ($\mathbf{1}_2^{2+}$: $[\mathbf{1}{\cdot}\mathbf{3}]^{2+}$: $\mathbf{3}_2^{2+}$) and thus close to the expected statistical intensities. If one takes the development of the heterodimer ion intensity as an example, one arrives at an estimate for the half-life of roughly 230 seconds.

12. ^{1}H NMR Spectra of a Mixture of $\mathbf{1_2}$·2PF$_6$ and $\mathbf{3_2}$·2PF$_6$

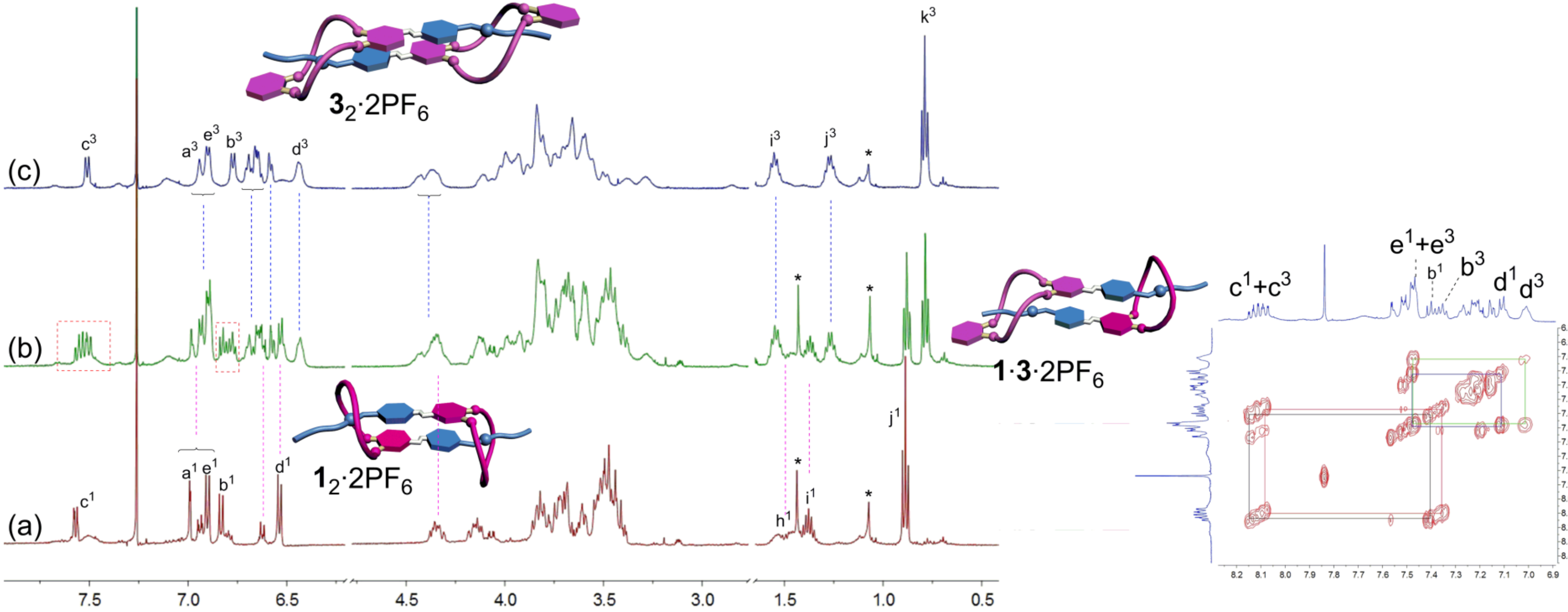

Figure S17. ^{1}H NMR spectra (500 MHz, $CDCl_3$:CD_3CN = 2:1, 10.0 mM, 298K) of (a) $\mathbf{1_2}$·2PF$_6$, (b) an equimolar mixture of $\mathbf{1_2}$·2PF$_6$ and $\mathbf{3_2}$·2PF$_6$ and (c) $\mathbf{3_2}$·2PF$_6$. Inset: partial ^{1}H-^{1}H COSY NMR spectrum of the mixture (8.2–6.9 ppm). Asterisks indicate solvent impurities. Dashed red boxes indicate spectral ranges in which clearly new signals attributable to the heterodimer are observed.

13. ESI mass spectra of a Mixture of $2\cdot\mathrm{PF}_6$ and $3_2\cdot 2\mathrm{PF}_6$

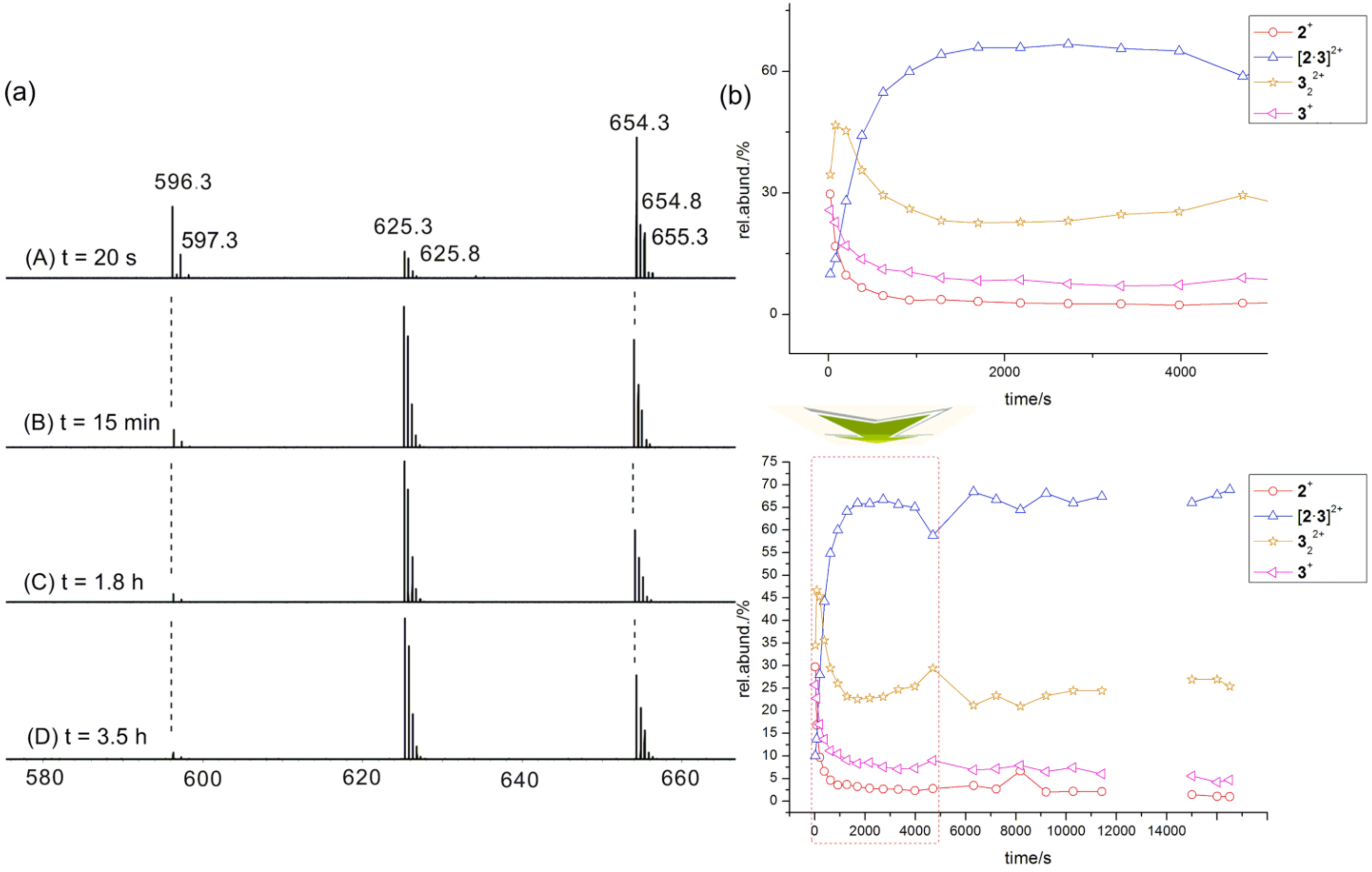

Figure S18. a) Mass spectra and b) time-plot of complex formation between $\mathbf{2}\cdot\mathrm{PF}_6$ and $\mathbf{3}_2\cdot\mathrm{PF}_6$. The hetero-[*c*2]daisy chain $[\mathbf{2}\cdot\mathbf{3}]^{2+}$ is the dominant species which develops again on a minute time scale.

14. ^{1}H NMR Spectra of a Mixture of $2{\cdot}PF_6$ and $3_2{\cdot}2PF_6$

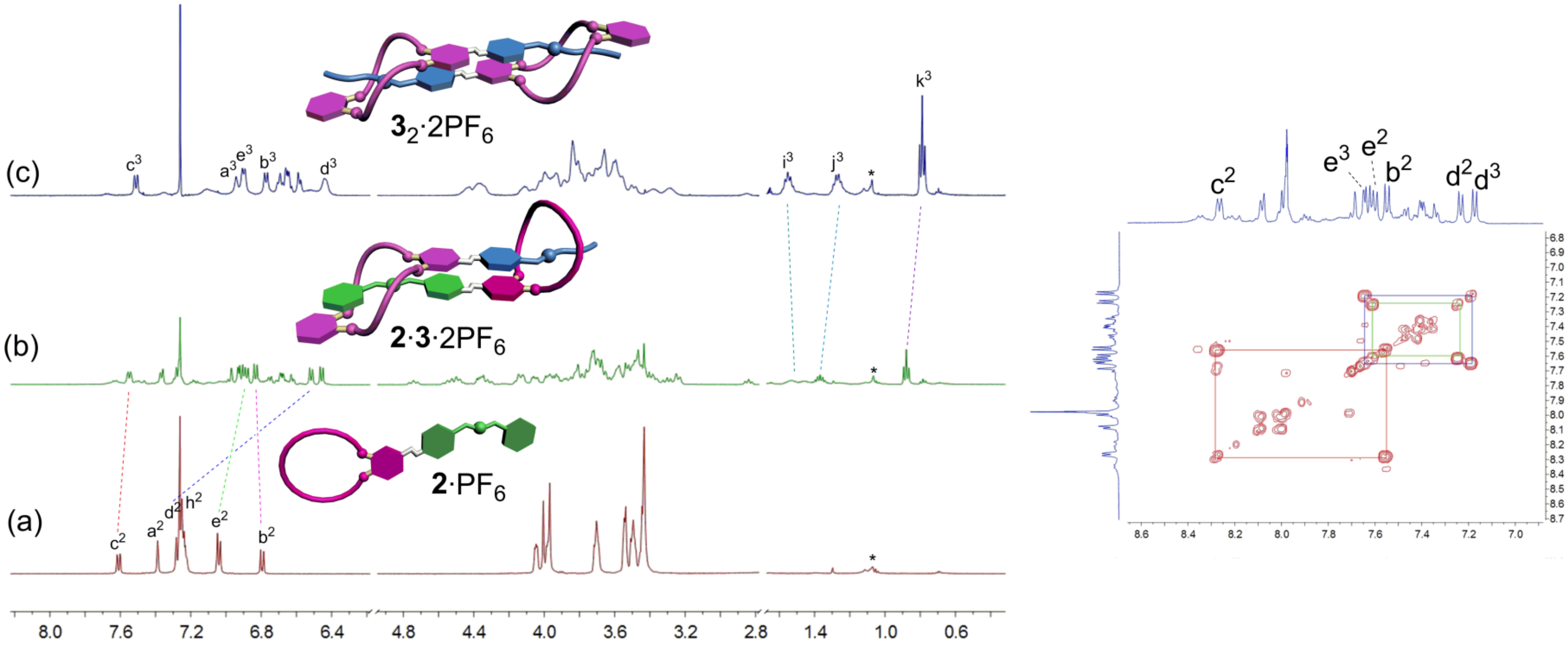

Figure S19. ^{1}H NMR spectra (500 MHz, CDCl$_3$:CD$_3$CN = 2:1, 10.0 mM, 298K) of (a) **2**·PF$_6$, (b) equimolar in monomer concentration of **2**·PF$_6$ and **3**$_2$·2PF$_6$ and (c) **3**$_2$·2PF$_6$. Inset: partial ^{1}H-^{1}H COSY NMR spectrum of the mixture (8.6–7.0 ppm). Asterisks indicate solvent impurities. The significant shifts of protons b^2, c^2, d^2 and e^2 of **2**·PF$_6$ and the shifts of protons h^3, i^3 and j^3 of **3**$_2$·2PF$_6$ indicate the formation of the hetero-[*c*2]daisy chain.

15. Ellipsoid plots of $3\cdot\mathrm{PF}_6$ and $4_2\cdot2\mathrm{PF}_6$